

Unilateral thalamic glioma disrupts large-scale functional architecture of human brain during resting state

This article was published in the following Dove Medical Press journal:
Neuropsychiatric Disease and Treatment

Sirui Li
Lei Gao
Ying Liu
Yawen Ao
Haibo Xu

Department of Radiology, Zhongnan
Hospital of Wuhan University, Wuhan
University, Wuhan 430071, People's
Republic of China

Background: The thalamus is an important deep brain structure for the synchronization of brain rhythm and the integration of cortical activity. Human brain imaging and computational modeling have non-invasively revealed its role in maintaining the cortical network architecture and functional hierarchy.

Purpose: The objective of this study was to identify the effect of unilateral thalamic damage on the human brain intrinsic functional architecture.

Patients and methods: We collected an 8-minute resting-state functional magnetic resonance imaging (R-fMRI) data on a 3.0 T magnetic resonance scanner for all the participants: a preoperative patient with left thalamus destroyed by anaplastic astrocytoma (WHO grade III type of astrocytoma) and 20 matched healthy controls. The R-fMRI data was analyzed for functional connectivity and amplitude of spontaneous fluctuations.

Results: The patient showed prominent decrease in functional connectivity within primary sensory networks and advanced cognitive networks, and extensive alterations in between-network coupling. Further analysis of the amplitude of spontaneous activity suggested significant decrease especially in the topographies of default mode network and the Papez circuit.

Conclusion: This result provided evidence about the consequences of thalamic destruction on the correlation and landscape of spontaneous brain activity, promoting our understanding of the effects of thalamic damage on large-scale brain networks.

Keywords: brain networks, functional connectivity, default mode network, Papez circuit

Introduction

Over the past decade, investigation of the human brain functional architecture and network neuroscience has been a major goal of neuroscience research.¹⁻⁴ Support for this connective perspective on brain function comes from studies of resting-state functional magnetic resonance imaging (R-fMRI), or intrinsic fluctuations of blood oxygen level dependent (BOLD) signal.⁵ Insights from the R-fMRI studies have brought out some functional attributes of human brain function, including large-scale intrinsic networks, and the temporal-spatial structure of the intrinsic BOLD signals.¹⁻⁴

The brain's repertoire of intrinsic functional architecture is ultimately determined by its structural underpinnings.^{6,7} Structural damage (such as those caused by stroke and tumor) often leads to varying degrees of brain dysfunction, depending on the change in topography and extent of the injury. Evidence based on computational neuroscience suggests that damage at the core/central nodes of human brain network, such as the anterior cingulate cortex, precuneus/posterior cingulate cortex, anterior insula, and the thalamus, often leads to collapse of the network.^{2,8-10}

Correspondence: Haibo Xu
Department of Radiology, Zhongnan
Hospital of Wuhan University, Wuhan
University, Wuhan 430071, People's
Republic of China
Email xuhaibo1120@hotmail.com

Out of all of these important core/central regions, the impact of thalamic damage on the functional architecture of the human brain is yet poorly understood. The thalamus is a primary relay station between the widespread cerebral cortex and subcortical regions, projects to almost all cortical and neocortical regions, maintains neuronal synchronization and well-organized functional networks, and integrates a wide range of cortical information to regulate consciousness, sleep, and wakefulness.^{8–11} Zhang et al¹² first mapped the intrinsic functional connectivity projection of specific thalamus sub-regions and the cerebral cortex, as well as developmental and maturation trajectories of the thalamocortical functional connectivity.¹³ One previous report focused its attention on the resting connectivity in a single multiple sclerosis patient with an anterior thalamic lesion, in particular in the default mode network (DMN).¹⁴ Unfortunately, despite the central role of the thalamus, information on the effect of the entire thalamic lesion on the brain's intrinsic activity is still extremely lacking. Thus, an important question arises: how does the destruction of the unilateral thalamus affect the functional operations of the human brain?

We hypothesized that thalamic destruction specifically results in dysfunction of the large-scale network and oscillations of intrinsic brain activity measured by R-fMRI. To explore this issue, we used a unique clinical case, a male patient with left thalamus destroyed by anaplastic astrocytoma (WHO grade III type of astrocytoma).

Methods

Ethics statement

The present study was approved by the Medical Ethics Committee of Zhongnan Hospital of Wuhan University, and written informed consent in accordance with the 1975 Declaration of Helsinki (and as revised in 1983) following a complete description of the measurement was obtained from all participants. The patient signed a written informed consent form that included permission to publish the case details and any accompanying images.

Subjects

A 30-year-old man was admitted to the hospital with a problem of headache and sleepiness since half a month. The patient complained of decreased vision and tinnitus, with decreased memory and distracted attention. He had no history of central nervous system infection, systemic disease, or congenital/chromosomal abnormality. Structural MRI demonstrated left thalamic space-occupying lesions, with long T1 and long T2 signals and a higher T2

fluid-attenuated inversion recovery (FLAIR) signal. A post-contrast T1-weighted scan revealed intra-focal partial/focal annular enhancement, while the rest did not enhance. The imaging characteristics indicated the diagnosis of glioma. Subsequently, the patient underwent thalamic tumor resection, and the postoperative pathology confirmed anaplastic astrocytoma (WHO grade III) (Figure 1). To establish differences between the individual case and its matched healthy controls, similar to the confidence interval reference range for establishing healthy controls, we carefully selected 20 healthy male controls (age range=19–45 years; mean age=31.2 years) with matched age and education. All subjects had normal hearing and vision and were right-handed as determined by the Edinburgh Handedness Inventory test.¹⁵

Functional MRI data acquisition

In all participants, T1 high-resolution anatomical and R-fMRI images were acquired on a Siemens Trio 3.0 T magnetic resonance scanner (Siemens, Munich, Germany). Head movement was restricted using a pillow and foam, and earplugs were used to attenuate scanner noise and maximize patient comfort. During the resting-state functional scans, all subjects were asked to close their eyes, stay awake, and remain as still as possible. A total of 8 minutes of T2*-weighted BOLD fMRI images were obtained (33 axial slices, 3.8-mm slice thickness with a 0.3-mm gap, 2-s recovery time (TR), 240 volumes). A T1 magnetization prepared rapid gradient echo sequence was also acquired in the same session for co-registration with functional data (176 sagittal slices, 1-mm in-plane resolution).

Preprocessing of fMRI data

R-fMRI data were processed using DPABI (rfmri.org/dpabi),¹⁶ Statistical Parametric Mapping (SPM12, <http://www.fil.ion.ucl.ac.uk>), and MATLAB (<https://www.mathworks.com>), and followed conventional methods as previously described.¹⁷ The methods mainly included the following steps: 1) discarding the first 10 TRs; 2) correcting for slice acquisition shifts; 3) realigning and correcting for small movements between scans, subjects with a maximum displacement in the x, y, or z direction of more than 2 mm or more than 2° of angular rotation about any axis for any of the 230 volumes were excluded from this study (no subject was excluded according to this criterion); 4) co-registering for individual T1 and the realigned functional volumes; 5) normalizing to the Montreal Neurological Institute (MNI152) space through Diffeomorphic Anatomical Registration Through Exponentiated Lie Algebra (DARTEL);¹⁸ 6) spatial smoothing (6 mm full-width half-maximum

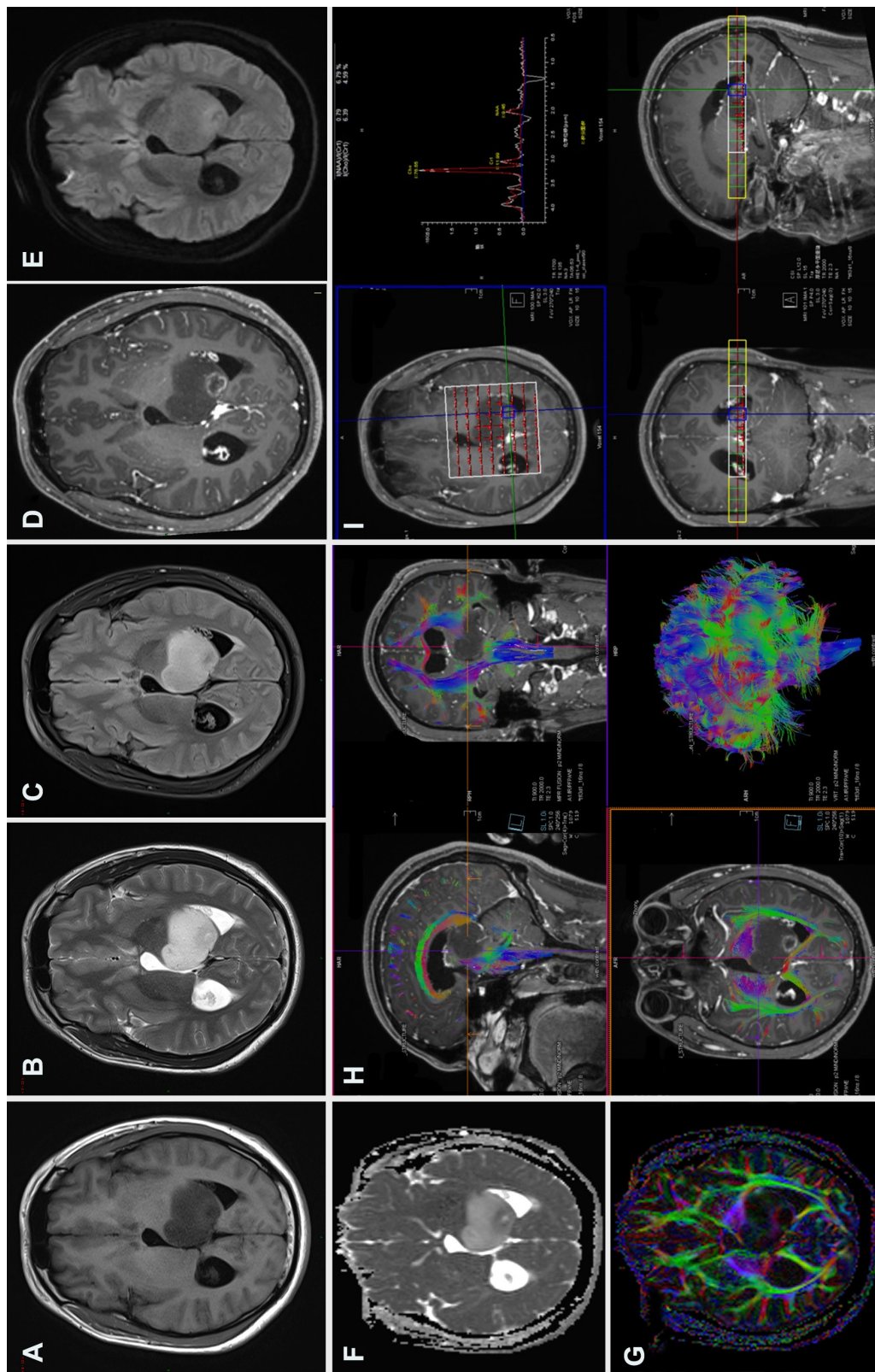


Figure 1 Brain MRI for the case. Conventional MRI sequences (A) T1WI, (B) T2WI, and (C) T2 FLAIR, left thalamic mass showed long T1, long T2, and higher T2-FLAIR signals, respectively; (D) contrast-enhanced T1WI sequence, small focal ring enhancement in the posterior part of the mass, no enhancement in the rest of the mass; (E) diffusion weighted imaging (DWI), b=1,000, a slightly higher ring signal in the dorsal mass; (F) ADC shows a slightly lower ring signal in the posterior mass, suggesting limited water diffusion; (G) A DTI sequence, FA map suggests that the left thalamic FA is significantly reduced compared with the contralateral side; (H) DTI fiber tractography, white matter fiber in the left thalamic lesion were destroyed or partial displacement; (I) MRS, left thalamic lesion enhancement area ROI metabolite spectrum, Cho increased significantly, NAA decreased significantly, Cho/NAA ratio of 8.09, and inverted lactate peak. The postoperative pathology confirmed the anaplastic astrocytoma (WHO grade III).

Abbreviations: ADC, apparent diffusion coefficient; Cho, choline; DTI, diffusion tensor imaging; FA, fractional anisotropy; FLAIR, fluid-attenuated inversion recovery; MRS, magnetic resonance spectroscopy; NAA, N-acetyl/aspartate; ROI, region of interest.

Gaussian blur in each direction); 7) reducing confounding factors via linear regression, including the signals from the white matter and cerebrospinal fluid and linear and quadratic trends; 8) temporal filtering (0.01–0.1 Hz) of the time series; and 9) motion scrubbing with a frame-wise displacement (FD) threshold of 0.5. The clean and low-frequency filtered resting functional volumes were used for further calculations. It should be noted that, for the patient, we made a left thalamic mask to avoid the influence of the lesion on the functional-structural registration.

Seed-based analysis

We began our analysis by computing seed-based functional connectivity. Based on our hypothesis and the patient's syndrome, we placed a set of seed regions on the healthy side (right hemisphere), including the default, dorsal attention, visual, auditory, salience, and the language systems, as previously described.^{19,20} The seeds were 6-mm-diameter spheres centered on previously published foci (Table 1).^{19,20} Functional connectivity maps were produced by extracting the BOLD time course from a seed region, and then computing the correlation coefficient between that time course and the time course from all other brain voxels.

ROI–ROI correlation analysis

To characterize the integrity and alterations of the large-scale functional brain architecture, we analyzed the region of interest (ROI)-wise functional connectivity. We selected twenty 6-mm spherical seed regions with the center coordinates on the dorsal attention, default, somatomotor, visual, auditory, and executive control networks (Table 2).¹⁹ The BOLD time series were extracted from each seed region, and then the correlation coefficients between the ROI pairs were calculated. The obtained correlation matrix which represented large-scale brain connectivity was then transformed using Fisher's z-shift for further individual versus group statistics.

Table 1 Seed regions and coordinates for seed-based analysis

System	Seed	Talairach coordinates (R)
Somatomotor	Right somatomotor	(39, –26, 51)
Default	Right posterior cingulate/precuneus	(4, –40, 43)
Language	Right inferior frontal gyrus	(48, –13, 31)
Visual	Right VI	(20, 75, 12)
Auditory	Right AI	(50, –25, 8)
Dorsal attention	Right intraparietal sulcus	(21, –69, 30)

Notes: System, seed name, and Talairach coordinates for seed regions used in this analysis are shown. These seed regions and coordinates were from Pizoli et al.²⁰

Abbreviation: R, right.

Table 2 Seed regions and coordinates for ROI-wise analysis

System	Seed	BA	Talairach coordinates (L) (R)
Dorsal attention	FEF	6	(–24, –12, 57) (28, –7, 54)
	IPS	7	(–23, –66, 46) (25, –58, 52)
	MT +	19/37	(–45, –69, –2) (45, –69, –4)
Default	MPF	32/10	(–3, 39, –2) (1, 54, 21)
	LP	39	(–47, –67, 36) (53, –67, 36)
	PCC	31	(–5, –49, 40)
Somatomotor	SM	4/3, 1, 2	(–39, –26, 51) (38, –26, 48)
Visual	VI	17	(–19.5, –75, 12) (16.5, –72, 12)
Auditory	AI	41	(–50, –25, 8) (50, –25, 8)
Executive control	dACC	32	(–1, 10, 46)
	OP		(–35, 14, 5) (36, 16, 4)

Notes: System, seed name, BA, and Talairach coordinates for seed regions used in this analysis are shown. These seed regions and coordinates were from Johnston et al.¹⁹

Abbreviations: BA, Brodmann's area; L, left; R, right; ROI, region of interest.

Amplitude of low-frequency fluctuations analysis

Finally, to analyze the effect of unilateral thalamic lesion on the local and whole brain spontaneous BOLD activity, we calculated the amplitude of the low frequency fluctuations (ALFF).²¹ ALFF mainly characterize the power of the low-frequency BOLD signal, which is supposed to indirectly reflect the extent or intensity of local intrinsic brain activity.^{16,21}

Statistical analysis

Since this study was for a single case analysis, we used an unpaired *t*-test with equal variance to examine the extent to which individual voxel and connectivity were deviated from its matched healthy controls. We defined the 95% confidence interval based on individual voxel and connectivity measures derived from healthy controls.

Results

Seed-based functional connectivity

Figure 2 depicts seed-based analysis, the seed regions settings, and seed-based functional connectivity profiles for the patient and healthy controls. The average correlation map of the seed-based functional connectivity of the healthy controls presents a characteristic layout consistent with previous reports. It can be found that the functional connectivity map of almost all six seed regions (right primary somatomotor, auditory, visual, intraparietal sulcus, inferior frontal gyrus, and posterior cingulate cortex) of the patient shows a decrease in functional connectivity, especially more prominent on the ipsilateral side of the patient's thalamic injury.

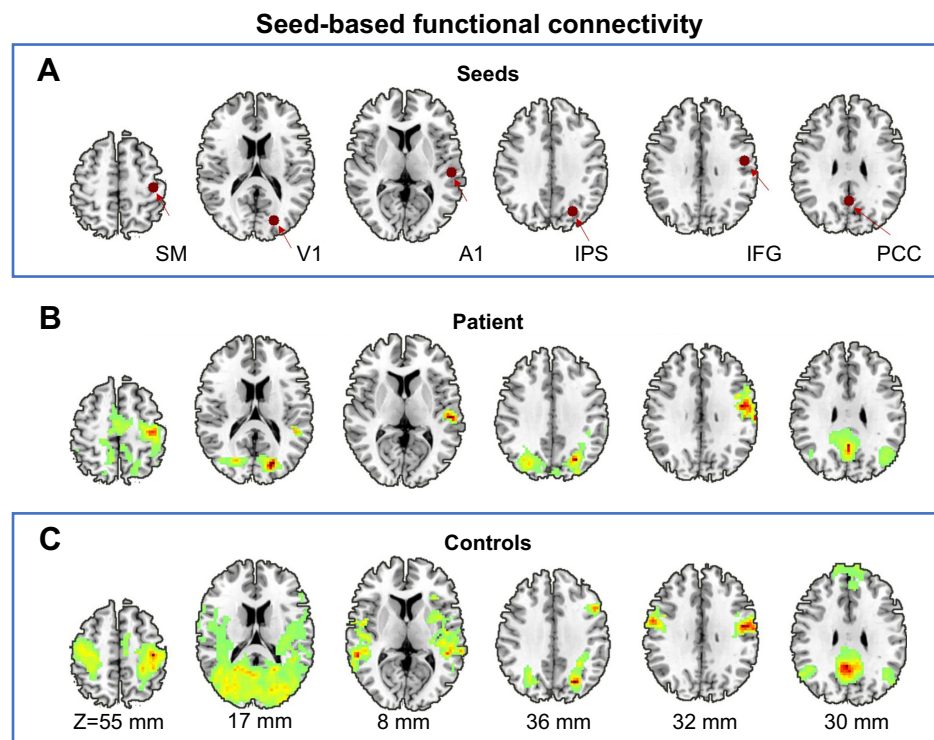


Figure 2 Seed-based functional connectivity. **(A)** Schematic of seed region selection, these 6-mm-diameter spherical regions include the right primary SM, A1, V1, IPS, IFG, and PCC, whose functional roles are involved in the somatomotor, auditory, visual, dorsal attention, language, and default systems, respectively. **(B)** The topographies where time courses in the patient's seed region is positively correlated ($r=0.5$) with other voxels in the whole brain, which are large-scale brain network systems including the somatomotor, auditory, visual, dorsal attention, language, and default systems; visually, these networks show prominent reductions in the contralateral functional connectivity corresponding to the seed regions (ie, ipsilateral functional connectivity). **(C)** Group average functional connectivity maps (correlation maps) of the healthy controls, the topographies where time courses in the seed region is positively correlated ($r=0.5$) with other voxels in the whole brain, outlines typical large-scale brain networks, as previous described and reported.

Abbreviations: A1, auditory; IFG, inferior frontal gyrus; IPS, intraparietal sulcus; PCC, posterior cingulate cortex; SM, somatomotor; V1, visual.

Pair wise ROI–ROI correlations

The patient and healthy controls' ROI-wise functional connectivity matrix and topographies are shown in Figure 3. Evidently, the controls showed typical connectional patterns of resting-state fluctuations within and between functional brain systems as previously reported. In contrast, the patient presented a less well-organized network architecture (Figure 3, right panel). Specifically, the connectivity matrix of the patient exhibited remarkably decreased functional connectivity within the default, salience, dorsal attention, and visual networks, and decreased functional connectivity between the salience and dorsal attention networks, as well as increased functional connectivity between default mode and salience networks.

Amplitude of low-frequency fluctuations analysis

Remarkable alterations in functional connectivity are seen, considering the nature of the thalamus in regulating cortical rhythm. We raised the question of whether the amplitude of the low frequency BOLD signal contributes to their

changes. To explore this issue, we then compared the difference between patient and controls in both voxel- and ROI-levels of ALFF. Gray matter-based voxel-level analysis showed significantly reduced ALFF in the patient in bilateral posterior cingulate gyri, bilateral hippocampus, anterior cingulate gyrus, bilateral lateral parietal, and temporal-parietal conjunctions (Figure 4). It is worth noting that these topographies largely overlapped with the default network (medial prefrontal cortex precuneus/posterior cingulate cortex, and bilateral lateral parietal cortices) and the so-called Papez circuit (hippocampal formation, fornix, mammillary bodies, mammillothalamic tract, anterior thalamic nucleus, cingulum, entorhinal cortex, hippocampal formation). The average ALFF values extracted from 46 classic cortical ROIs also suggest a significantly uniform ALFF reduction within the default network, and isolated nodes from other systems (Figure 5).

Discussion

Non-invasive MR human brain imaging brings an unprecedented opportunity to understand the human brain architecture.

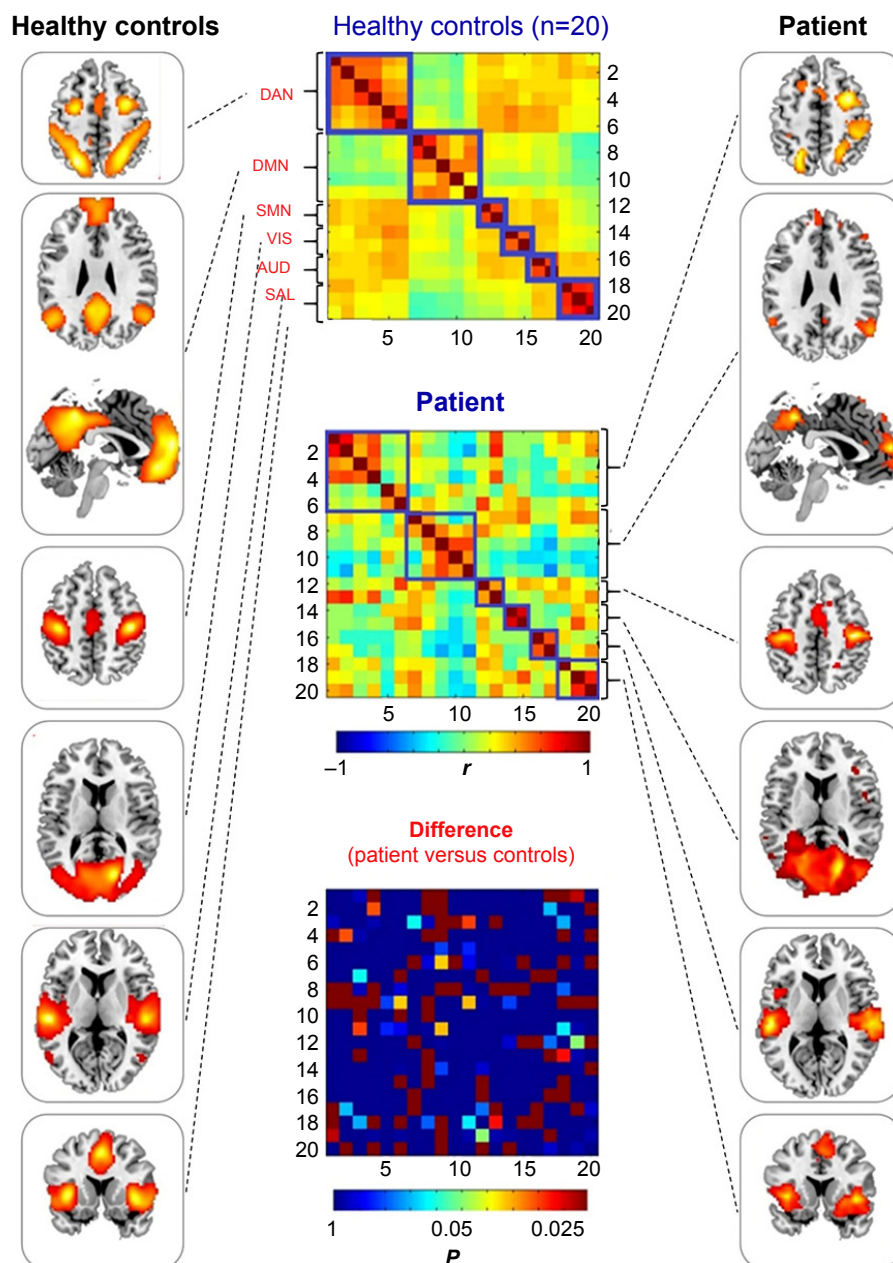


Figure 3 ROI-based large-scale brain networks. Left panel: group average of ROI-based functional connectivity in healthy controls, topographies of large-scale brain networks including dorsal attention, default, somatomotor, visual, auditory, and salience systems from top to bottom. Middle panel: functional connectivity matrices (20 nodes x 20 nodes correlation) of healthy controls' mean (top), patient (middle), and between-group difference in patient versus controls comparison via Z-transformation (bottom, the elements in this matrix have been transformed into corrected P -values, with only $P \leq 0.05$ coloring, and $P > 0.05$ colored with uniform dark blue). Right panel: ROI-based functional connectivity in the patient, topographies of large-scale brain networks including dorsal attention, default, somatomotor, visual, auditory, and salience systems from top to bottom.

Abbreviations: AUD, auditory network; DAN, dorsal attention network; DMN, default mode network; ROI, region of interest; SAL, salience network; SMN, somatomotor network; VIS, visual network.

One of the important research domains is the relationship between human brain structure and function. Empirical data and computational neuroscience have revealed that, in complex human brain networks, some hub nodes are critical for maintaining the integrity and dynamics of the functional architecture. In this study, we presented a case to investigate how the damage of the unilateral thalamus would affect the large-scale resting of the human brain.

Using an 8-minute scan of resting-state fMRI data, we analyzed the spontaneous brain activity architecture from three levels: 1) seed-based univariate analysis of a given network within and between hemispheric functional connectivity, 2) large-scale cortical network based on ROI pairs correlations, and 3) amplitude and distribution of these spontaneous neural activities. Consistent with our hypothesis, unilateral thalamic injury significantly reduced

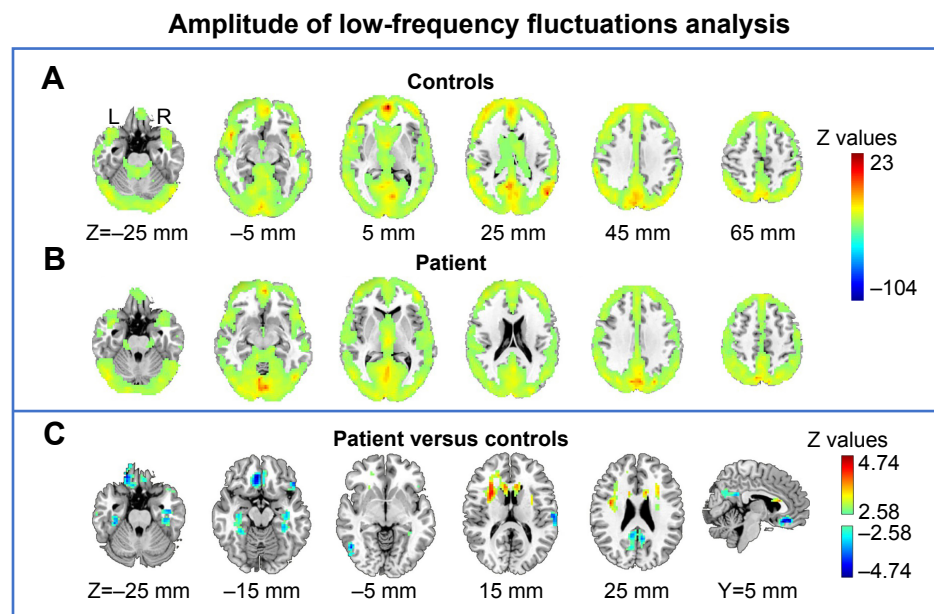


Figure 4 Amplitude of low-frequency fluctuations analysis. (A) Average gray matter resting fluctuations amplitude in the healthy controls. (B) Gray matter resting fluctuations amplitude in the patient. (C) Between-group comparison of patient versus controls via Z-transformation.

Note: Y and Z represent sagittal and axial coordinates, respectively, in standard brain template space.

Abbreviations: L, left; R, right.

functional connectivity in the sensory (visual, auditory, and somatomotor) and cognitive networks (dorsal attention, default, and salience), meanwhile suppressed cortical spontaneous BOLD fluctuations were also found in this patient.

Effects of thalamic lesions on resting-state functional connectivity

Thalamic injury significantly disrupts the large-scale neuronal networks (the canonical signature of low-frequency

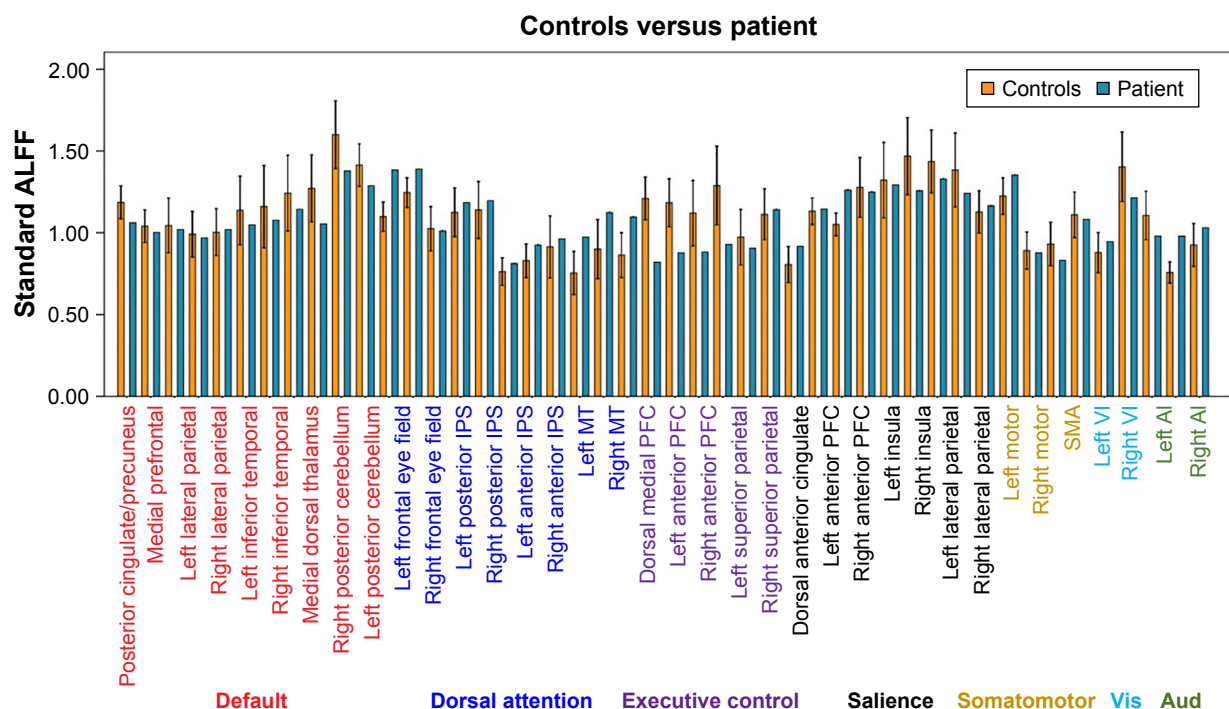


Figure 5 ALFF signals over predefined ROIs. The average values in the patient (blue) and controls (orange) across 46 6-mm-diameter spherical canonical ROIs (all in gray matter),²⁰ corresponding to previously described nodes within the default, dorsal attention, executive control, salience, somatomotor, primary visual, as well as primary auditory networks (labeled in the bottom panel). The error bars indicate 95% confidence interval for the ALFF values derived from the healthy controls.

Abbreviations: AI, auditory; ALFF, amplitude of the low frequency fluctuations; IPS, intraparietal sulcus; MT, middle temporal region; PFC, prefrontal cortex; ROI, region of interest; VI, visual.

fluctuations patterns), which mostly reduce within and between the brain network systems. One previous study has also focused its attention on resting connectivity between a single multiple sclerosis patient with an anterior thalamic lesion and a group of controls, in particular, in the default mode network.¹⁴ In this particular case of our study, we presented a complete glioma-induced left thalamic destruction that extended the range of damage, and thus the damage spectrum spanned the default network and involved multiple large-scale brain networks of both advanced cognitive functional networks and primary sensory networks. Widespread reduction in cortical functional connectivity is thought to be responsible for communication and goal-directed behavioral disorders, including physical disconnection caused by traumatic brain injury,²² reduced occipital inputs due to early blindness,²³ reduced sensory motor functionality in early stage limb-onset amyotrophic lateral sclerosis,²⁴ and the multi-dimensional sensory abnormalities caused by acute infarction or bleeding of the unilateral posterolateral thalamus.¹⁴

The thalamus is an important node on the basal ganglia circuitry,⁸ it not only promotes the transmission of almost all cortical inputs, including primary sensory, and advanced cognitive functions but also facilitates the regulation and integration of this information. Cortical-thalamic-cortical loops are another important way for the thalamus to function, promoting sensorimotor and advanced cognitive input information to the neocortex.^{9,11,25} Previous functional¹² and diffusion²⁶ MRI have established functional connectivity and fiber tracking projections of the thalamus-cortex. Based on these findings, prominent changes were reported in various physiological states,²⁷ development,^{13,28,29} and brain diseases.^{30–32}

Altered resting spontaneous activity

The widespread reduction in cortical functional connectivity raised a question whether that may reflect changes in the information propagation by the thalamic gating, and we continued to investigate the amplitude of this spontaneous neural activity (ie, the ALFF). We found that the overall ALFF in the patient's gray matter ROIs was generally lower than the mean of the healthy controls +2 standard deviations. Further voxel-based statistical analysis found that the topographies of the patient with significantly reduced ALFF included posterior cingulate gyrus, bilateral hippocampus, anterior cingulate gyrus, bilateral lateral parietal and temporal-parietal conjunctions. It is worth noting that these topographies largely overlapped with the default network and the so-called Papez circuit.

On the other hand, results of the ALFF analysis are from those of functional connectivity, whose findings involved multiple large-scale brain networks. One main reason may be that the unilateral thalamic lesion disrupts the subcortical information outputs and cortical communication and integration, leading to frequency changes in neuronal assembly oscillations.

The default brain network was traditionally found to be a negative activation while performing goal-directed tasks, possibly as a baseline activity at rest.³³ Later clinical applications in the neuroimaging community have found characteristic changes (mainly reduced) of the default network in memory impairment-associated conditions including Alzheimer's disease, altered coupling of default network, and other large-scale networks in attention deficit hyperactivity disorder and autism (for a systemic review, please see Raichle³). Especially in the past decade, graph theory analysis (based on human brain connectome data) and cluster analysis have identified that DMN is at the core of the human brain functional hierarchy.² Recent studies have recognized lag structure in the human intrinsic architecture, the DMN is supposed to be an early spatiotemporal source, promoting the propagation of neural information to other large-scale cortical networks (later spatiotemporal sources).^{4,34} A number of previous studies have reported focally reduced ALFF in various neuropsychiatric conditions.^{35,36} It is highly likely that these effects are related to the decreased local activity and shifted frequency band.^{37,38} In summary, ALFF anomalies mainly occur in the DMN and the Papez circuit as these regions may serve as a source of spontaneous signaling, mediating the integration of other sensory and cognitive networks, cortical rhythms of inhibitory control, and coordination.

This report has important clinical implications, as previous studies have focused on intact brain and animal experiments in the thalamus. This study provides insight into understanding the effects of unilateral thalamic destruction on the amplitude and correlation patterns (connectivity) of resting spontaneous neural activity. Thalamic stimulation therapy for disorders, Parkinson's disease, etc. provides theoretical evidence, and also provides a potentially useful tool for understanding its targeted stimulation.

Conclusion

Unilateral thalamic damage suppresses the amplitude of spontaneous neuronal activity, especially in the default network and Papez circuit, as well as the integrity and coupling of large-scale functional networks, and functional connectivity within the ipsilateral side of injury. This result provided evidence about the consequences of thalamic destruction on

the correlation and landscape of spontaneous brain activity, thus promoting our understanding of the effects of thalamic damage on large-scale brain networks.

Acknowledgments

This study has been supported by the National Natural Science Foundation of China (under Grant Nos 81771819 and 81571734), National key research and development plan of China (Project 2017YFC0108803), Zhongnan Hospital of Wuhan University Science, Technology and Innovation Seed Fund (Projects cxy2017048 and cxy20160057), and the Fundamental Research Funds for the Central Universities (Projects 2042017kf0284 and 2016060605100525). We thank all members of the Departments of Radiology and Neurosurgery at Zhongnan Hospital of Wuhan University for conducting this study as well as all participants for their good collaboration.

Author contributions

SL, LG, and YL planned and conducted statistical analyses, wrote the draft of the manuscript including creation of the figures, and modified all subsequent drafts. LG processed all MRI data. HX designed the study. YL and YA reviewed the final draft of the manuscript. SL and YA collected the MRI data. HX supervised data analyses, substantially contributed to interpretation of the results, and made substantial modifications to all drafts of the manuscript. All authors contributed to data analysis, drafting and revising the article, gave final approval of the version to be published, and agree to be accountable for all aspects of the work.

Disclosure

The authors declare no potential conflicts of interest with respect to the research, authorship, and/or publication of this article. The authors report no other conflict of interest in this work.

References

- Mitra A, Raichle ME. How networks communicate: propagation patterns in spontaneous brain activity. *Philos Trans R Soc Lond B Biol Sci*. 2016;371(1705):20150546. doi:10.1098/rstb.2015.0546
- Bassett DS, Sporns O. Network neuroscience. *Nat Neurosci*. 2017;20(3):353. doi:10.1038/nn.4465
- Raichle ME. The brain's default mode network. *Annu Rev Neurosci*. 2015;38:433–447. doi:10.1146/annurev-neuro-071013-014030
- Raichle ME. The restless brain: how intrinsic activity organizes brain function. *Philos Trans R Soc Lond B Biol Sci*. 2015;370(1668):20140172. doi:10.1098/rstb.2014.0172
- Biswal B, Zerrin Yetkin F, Haughton VM, Hyde JS. Functional connectivity in the motor cortex of resting human brain using echo-planar MRI. *Magn Reson Med*. 1995;34(4):537–541.
- Honey CJ, Sporns O, Cammoun L, et al. Predicting human resting-state functional connectivity from structural connectivity. *Proc Natl Acad Sci*. 2009;106(6):2035–2040. doi:10.1073/pnas.0811168106
- Greicius MD, Supekar K, Menon V, Dougherty RF. Resting-state functional connectivity reflects structural connectivity in the default mode network. *Cereb Cortex*. 2009;19(1):72–78. doi:10.1093/cercor/bhn059
- Postuma RB, Dagher A. Basal ganglia functional connectivity based on a meta-analysis of 126 positron emission tomography and functional magnetic resonance imaging publications. *Cereb Cortex*. 2006;16(10):1508–1521. doi:10.1093/cercor/bhj088
- Sherman SM, Guillery RW. *Exploring the Thalamus and Its Role in Cortical Function*. 2nd ed. Cambridge, Massachusetts. London, England: The MIT Press; 2006.
- Buzsaki G, Draguhn A. Neuronal oscillations in cortical networks. *Science*. 2004;304(5679):1926–1929. doi:10.1126/science.1099745
- Sherman SM. The thalamus is more than just a relay. *Curr Opin Neurobiol*. 2007;17(4):417–422. doi:10.1016/j.conb.2007.07.003
- Zhang D, Snyder AZ, Shimony JS, Fox MD, Raichle ME. Noninvasive functional and structural connectivity mapping of the human thalamo-cortical system. *Cereb Cortex*. 2009;20(5):1187–1194. doi:10.1093/cercor/bhp182
- Fair D, Bathula D, Mills KL, et al. Maturing thalamocortical functional connectivity across development. *Front Syst Neurosci*. 2010;4:10. doi:10.3389/fnsys.2010.00009
- Jones DT, Mateen FJ, Lucchinetti CF, Jack CJ, Welker KM. Default mode network disruption secondary to a lesion in the anterior thalamus. *Arch Neurol*. 2011;68(2):242–247. doi:10.1001/archneurol.2010.259
- Oldfield RC. The assessment and analysis of handedness: the Edinburgh inventory. *Neuropsychologia*. 1971;9(1):97–113.
- Yan C, Wang X, Zuo X, Zang Y. DPABI: data processing & analysis for (resting-state) brain imaging. *Neuroinformatics*. 2016;14(3):339–351. doi:10.1007/s12021-016-9299-4
- Li J, Gao L, Xie K, et al. Detection of functional homotopy in traumatic axonal injury. *Eur Radiol*. 2017;27(1):325–335. doi:10.1007/s00330-016-4302-x
- Ashburner J. A fast diffeomorphic image registration algorithm. *Neuroimage*. 2007;38(1):95–113. doi:10.1016/j.neuroimage.2007.07.007
- Johnston JM, Vaishnavi SN, Smyth MD, et al. Loss of resting inter-hemispheric functional connectivity after complete section of the corpus callosum. *J Neurosci*. 2008;28(25):6453–6458. doi:10.1523/JNEUROSCI.0573-08.2008
- Pizoli CE, Shah MN, Snyder AZ, et al. Resting-state activity in development and maintenance of normal brain function. *Proc Natl Acad Sci U S A*. 2011;108(28):11638–11643. doi:10.1073/pnas.1109144108
- Yu-Feng Z, Yong H, Chao-Zhe Z, et al. Altered baseline brain activity in children with ADHD revealed by resting-state functional MRI. *Brain Dev*. 2007;29(2):83–91. doi:10.1016/j.braindev.2006.07.002
- Mayer AR, Mannell MV, Ling J, Gasparovic C, Yeo RA. Functional connectivity in mild traumatic brain injury. *Hum Brain Mapp*. 2011;32(11):1825–1835. doi:10.1002/hbm.21151
- Liu Y, Yu C, Liang M, et al. Whole brain functional connectivity in the early blind. *Brain*. 2007;130(Pt 8):2085–2096. doi:10.1093/brain/awm121
- Agosta F, Valsasina P, Absinta M, et al. Sensorimotor functional connectivity changes in amyotrophic lateral sclerosis. *Cereb Cortex*. 2011;21(10):2291–2298. doi:10.1093/cercor/bhr002
- Sherman SM. Functioning of circuits connecting thalamus and cortex. *Compr Physiol*. 2017;7:713–739. doi:10.1002/cphy.c160032
- Behrens TE, Johansen-Berg H, Woolrich MW, et al. Non-invasive mapping of connections between human thalamus and cortex using diffusion imaging. *Nat Neurosci*. 2003;6(7):750. doi:10.1038/nn1075
- Shao Y, Wang L, Ye E, et al. Decreased thalamocortical functional connectivity after 36 hours of total sleep deprivation: evidence from resting state fMRI. *PLoS One*. 2013;8(10):e78830. doi:10.1371/journal.pone.0078830
- Anticevic A, Haut K, Murray JD, et al. Association of thalamic dysconnectivity and conversion to psychosis in youth and young adults at elevated clinical risk. *Am J Psychiatry*. 2015;172(9):882–891. doi:10.1001/jamapsychiatry.2015.0566

29. Alcauter S, Lin W, Smith JK, et al. Development of thalamocortical connectivity during infancy and its cognitive correlations. *J Neurosci*. 2014;34(27):9067–9075. doi:10.1523/JNEUROSCI.0796-14.2014
30. Woodward ND, Karbasforoushan H, Heckers S. Thalamocortical dysconnectivity in schizophrenia. *Am J Psychiatry*. 2012;169(10):1092–1099. doi:10.1176/appi.ajp.2012.12010056
31. Anticevic A, Cole MW, Repovs G, et al. Characterizing thalamocortical disturbances in schizophrenia and bipolar illness. *Cereb Cortex*. 2013;24(12):3116–3130. doi:10.1093/cercor/bht165
32. Nair A, Treiber JM, Shukla DK, Shih P, Müller R. Impaired thalamocortical connectivity in autism spectrum disorder: a study of functional and anatomical connectivity. *Brain*. 2013;136(6):1942–1955. doi:10.1093/brain/awt079
33. Raichle ME, MacLeod AM, Snyder AZ, Powers WJ, Gusnard DA, Shulman GL. A default mode of brain function. *Proc Natl Acad Sci*. 2001;98(2):676–682. doi:10.1073/pnas.98.2.676
34. Mitra A, Snyder AZ, Hacker CD, Raichle ME. Lag structure in resting-state fMRI. *J Neurophysiol*. 2014;111(11):2374–2391. doi:10.1152/jn.00804.2013
35. Yan X, Brown AD, Lazar M, et al. Spontaneous brain activity in combat related PTSD. *Neurosci Lett*. 2013;547:1–5. doi:10.1016/j.neulet.2013.04.032
36. Boyer A, Deverdun J, Duffau H, et al. Longitudinal changes in cerebellar and thalamic spontaneous neuronal activity after wide-awake surgery of brain tumors: a resting-state fMRI study. *Cerebellum*. 2016;15(4):451–465. doi:10.1007/s12311-015-0709-1
37. Gao L, Bai L, Zhang Y, et al. Frequency-dependent changes of local resting oscillations in sleep-deprived brain. *PLoS One*. 2015;10(3):e120323.
38. Zhou F, Huang S, Zhuang Y, Gao L, Gong H. Frequency-dependent changes in local intrinsic oscillations in chronic primary insomnia: a study of the amplitude of low-frequency fluctuations in the resting state. *NeuroImage Clin*. 2017;15:458–465. doi:10.1016/j.nicl.2016.05.011

Neuropsychiatric Disease and Treatment

Dovepress

Publish your work in this journal

Neuropsychiatric Disease and Treatment is an international, peer-reviewed journal of clinical therapeutics and pharmacology focusing on concise rapid reporting of clinical or pre-clinical studies on a range of neuropsychiatric and neurological disorders. This journal is indexed on PubMed Central, the 'PsycINFO' database and CAS,

and is the official journal of The International Neuropsychiatric Association (INA). The manuscript management system is completely online and includes a very quick and fair peer-review system, which is all easy to use. Visit <http://www.dovepress.com/testimonials.php> to read real quotes from published authors.

Submit your manuscript here: <http://www.dovepress.com/neuropsychiatric-disease-and-treatment-journal>